Flipping and scooping of curved 2D rigid fibers in simple shear: the Jeffery equations

Darren Crowdy[1, a)]

Department of Mathematics, Imperial College London, 180 Queen's Gate, London SW7 2AZ, UK.

(Dated: 20 April 2016)

The dynamical system governing the motion of a curved rigid two-dimensional circular-arc fiber in simple shear is derived in analytical form. This is achieved by finding the solution for the associated low-Reynolds-number flow around such a fiber using the methods of complex analysis. Solutions of the dynamical system display the "flipping" and "scooping" recently observed in computational studies of three-dimensional fibers using linked rigid rod and bead-shell models [Wang *et al*, *Phys. Fluids*, **24**, (2012)]. To complete the Jeffery-type equations for a curved fiber in a linear flow field we also derive its evolution equations in an extensional flow. It is expected that the equations derived here also govern the motion of slender, curved, three-dimensional rigid fibers when they evolve purely in the plane of shear or strain.

Keywords: Jeffery orbits, curved fiber, fluid-structure interaction, suspension dynamics

[a)]Electronic mail: d.crowdy@imperial.ac.uk

I. INTRODUCTION

To understand the dynamics and bulk properties of particle suspensions it is of great importance to study the dynamics of isolated particles at low Reynolds number in basic flows such as simple shear. Work on this fundamental fluid dynamical problem dates back to the seminal work of Jeffery[1] on the shear-induced motion of rigid force and torque-free ellipsoids; in that case, the governing dynamical system can be written down in closed form with those ordinary differential equations now commonly referred to as "the Jeffery equations", and their solutions "the Jeffery orbits". Important contributions for more general geometries are due to Bretherton[2] (who showed that features of Jeffery's analysis carry over to more general axisymmetric particles) and Hinch & Leal[5] (who studied non-axisymmetric particles). Investigations of other particle types in simple shear have been performed by Skjetne, Ross & Klingenberg[6], Yarin, Gottlieb & Roisman[7] and Makino & Doi[8] in some cases incorporating the effects of deformability of the particles. Information on the dynamical behaviour of isolated particles is important in that it serves as the microscopic model input to mean-field models of general suspension dynamics[9–11]. Background on fluid-structure interactions of this general type can be found in Chapters 2–5 of a recent monograph editted by Duprat & Stone[4].

Beyond spheres and ellipsoids, the study of thin fibers and rods in suspension has been the subject of much recent research involving mainly computational simulations of both isolated and interacting particles[12–17]. Applications include the manufacture of paper products, the study of polymer melts as well as various fiber-reinforced composite materials. The dynamics of thin fibers in suspension is a function not only of hydrodynamical interactions but also the compliant nature of the suspended particles; the nature of the ambient flow is also important, with both simple shear and extensional flows constituting basic paradigms. Manikantan & Saintillan[16] have recently performed computational investigations of how a single flexible polymer filament behaves in an extensional flow. More complex ambient flows are also of interest and, in a combined experimental and theoretical study, Quennouz *et al*[17] have looked at single elastic filament evolution in a cellular matrix of electromagnetically driven recirculating vortices.

Even for a single particle, in preparation for a study of the full fluid-structure interaction problem for flexible fibers, it is natural to first gain a full understanding of the hydrodynamics

of a single *rigid* rod-like particle in simple flows. With this aim, Wang, Tozzi, Graham & Klingenberg[15] recently performed a computational study of the dynamics of isolated curved, rigid, non-chiral fibers in simple shear; they employed both a linked rigid rod model and a bead-shell model to carry out their study. Among the results it was observed that when a fiber evolves in the plane of shear it engages in motions the authors refer to as "flipping" and "scooping". For more general out-of-plane motions a drift phenomenon is observed that results from a coupling of the rotational and translational dynamics, and the combined effects of the flipping, scooping, and spinning motions of the fiber.

The present work is inspired by that of Wang, Tozzi, Graham & Klingenberg[15]; it complements their computational study in providing a complete analytical characterization of the motion of curved rigid *two-dimensional* fibers in simple shear. We choose to refer to the objects studied here as 2D *fibers* but, when embedded in 3D, the 2D fibers considered here are really three-dimensional "sheets" extending indefinitely in the third dimension (perpendicular to the plane of shear). The two-dimensional scenario is of less direct physical relevance, but the investigation is valuable: first, the study gives useful theoretical insights into the 3D problem and, indeed, the explicit dynamical system we find exhibits precisely the aforementioned "flipping" and "scooping" phenomena already observed in direct numerical simulations[15]; second, an explicit Jeffery-type dynamical system for slender, curved, rigid 3D fibers is not currently known but it is reasonable to expect that those evolving purely in the plane of shear (or strain) will satisfy exactly the same evolution equations as our 2D fibers. Indeed we start by showing that this is true for *straight* fibers.

Our main results can be summarized as follows. If, as shown in Figure 1, the midpoint of a curved 2D rigid fiber is at $(x_c(t), y_c(t))$ and its orientation angle relative to the positive x-axis is $\phi(t)$ we show that the Jeffery-type dynamical system for the evolution of these parameters in simple shear with shear rate $\dot{\gamma}$ having the far-field form $(u, v) \sim (\dot{\gamma}y, 0)$ is given by

$$\begin{aligned}
\frac{dx_c}{dt} &= \dot{\gamma}y_c - \frac{\dot{\gamma}R}{2}\left[1 - \cos^4\left(\frac{L}{4R}\right)\right]\cos\phi, \\
\frac{dy_c}{dt} &= \frac{\dot{\gamma}R}{2}\left[1 - \cos^4\left(\frac{L}{4R}\right)\right]\sin\phi, \\
\frac{d\phi}{dt} &= -\frac{\dot{\gamma}}{2} + \frac{\dot{\gamma}}{2}\cos^2\left(\frac{L}{4R}\right)\cos 2\phi,
\end{aligned} \tag{1}$$

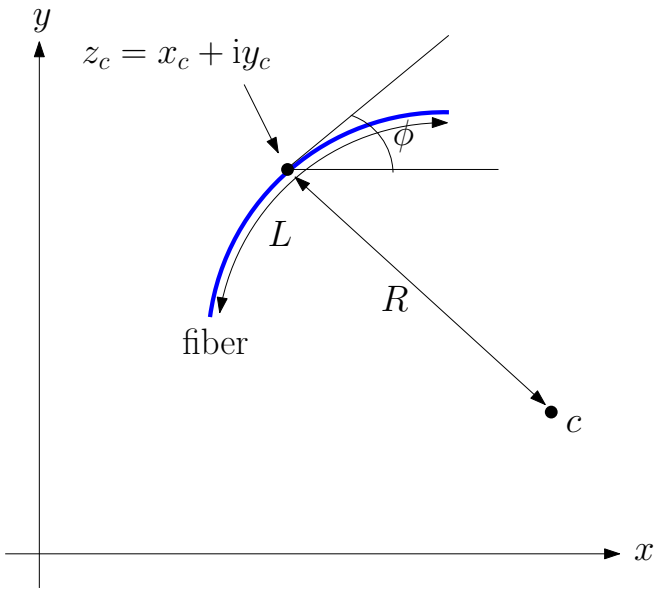


FIG. 1. Schematic of a curved rigid two-dimensional fiber in the (x, y)-plane with midpoint at (complex) location $z_c = x_c + \mathrm{i}y_c$. The angle ϕ gives its orientation relative to the positive x-axis. The fiber is a circular arc of length L and radius of curvature is R. Since the fiber is rigid the latter are fixed in time.

where L is the fiber length and R is its radius of curvature. In §II we describe the complex variable formulation of two-dimensional Stokes flow used to derive (1). §III includes details of an instructive first case study of the well-known straight fiber case then, in §IV, that analysis is generalized in a natural way to curved fibers. §V explores the dynamics encoded in system (1).

To complete our study of the Jeffery-type equations for a 2D curved circular-arc fiber in an ambient linear flow in §VI we also give the derivation of the system

$$\begin{aligned}
\frac{dx_c}{dt} &= \dot{\delta} x_c + \dot{\delta} R \left[1 - \cos^4\left(\frac{L}{4R}\right)\right] \sin\phi, \\
\frac{dy_c}{dt} &= -\dot{\delta} y_c + \dot{\delta} R \left[1 - \cos^4\left(\frac{L}{4R}\right)\right] \cos\phi, \\
\frac{d\phi}{dt} &= -\dot{\delta} \cos^2\left(\frac{L}{4R}\right) \sin 2\phi
\end{aligned} \tag{2}$$

which describes the evolution of the same fiber in an extensional flow having the far-field form $(u, v) \sim (\dot{\delta} x, -\dot{\delta} y)$ where $\dot{\delta}$ is the strain rate.

One immediate observation, on inspection of (1) and (2), is that curvature effects manifest themselves in the dynamics only through the non-dimensional parameter $\cos^2(L/4R)$.

II. COMPLEX VARIABLE FORMULATION

For two-dimensional incompressible Stokes flow advantage can be taken of a complex variable formulation of the mathematical problem. On combining this with conformal mapping techniques we will show that it is possible to solve the problems of interest here in analytical form. Mathematically, the method we employ is a variant of that used by Crowdy & Samson[3] to study various Stokes flows past gaps in a wall.

With inertia ignored, at each instant in time the streamfunction $\psi(x, y)$ associated with an incompressible two-dimensional Stokes flow of a fluid of viscosity μ around a two-dimensional rigid fiber satisfies the biharmonic equation

$$\nabla^4 \psi = 0, \tag{3}$$

where the fluid velocity components are then $(u, v) = (\partial\psi/\partial y, -\partial\psi/\partial x)$ and ∇^2 is the two-dimensional Laplacian operator. On introducing the complex variable $z = x + \mathrm{i}y$ the general solution to (3) can be represented by

$$\psi(x, y) = \mathrm{Im}[\overline{z} f(z) + g(z)], \tag{4}$$

where $f(z)$ and $g(z)$ are two analytic functions in the fluid region; they are sometimes called *Goursat functions*. If p denotes the fluid pressure then it can be shown[18,19] that

$$\frac{p}{\mu} - \mathrm{i}\omega = 4f'(z), \qquad u - \mathrm{i}v = -\overline{f(z)} + \overline{z} f'(z) + g'(z), \qquad e_{11} + \mathrm{i}e_{12} = z\overline{f''(z)} + \overline{g''(z)}, \tag{5}$$

where ω is the fluid vorticity and

$$e_{ij} = \frac{1}{2}\left(\frac{\partial u_i}{\partial x_j} + \frac{\partial u_j}{\partial x_i}\right) \tag{6}$$

is the fluid rate-of-strain tensor. The prime notation is used to express derivatives with respect to the argument of the function. Using these results the complex form of the fluid stress on the boundary, i.e.,

$$-pn_i + 2\mu e_{ij} n_j, \tag{7}$$

where n_i denote the components of the surface normal can be shown to be

$$2\mu \mathrm{i}\frac{dH}{ds}, \qquad H(z,\overline{z}) \equiv f(z) + z\overline{f'(z)} + \overline{g'(z)}, \tag{8}$$

where s denotes arclength along the boundary. Crowdy & Tanveer[19] give more details of the derivation of (8). It is easy to check that the simple transformation

$$f(z) \mapsto f(z) + a, \qquad g'(z) \mapsto g'(z) + \overline{a}, \tag{9}$$

where a is some complex constant can be seen to leave the velocity and stress fields invariant which can be interpreted to mean that there is an additive degree of freedom in the specification of $f(z)$, say.

The main challenge is to find $f(z)$ and $g(z)$ for the problem of a force-free and torque-free fiber in a simple shear flow so that, as $|z| \to \infty$,

$$(u, v) \sim (\dot{\gamma} y, 0), \tag{10}$$

where $\dot{\gamma}$ is the far-field shear rate. Strictly speaking, since the fiber midpoint and orientation evolve in time, the Goursat functions will depend on time and should really be denoted by $f(z,t)$ and $g(z,t)$ but, for brevity, we omit any such explicit time dependence in our notation. This choice is natural in view of the quasi-steady nature of the problem.

The relation in (5) for $u - \mathrm{i}v$ can be used to establish that we must have

$$f(z) \sim \frac{\mathrm{i}\dot{\gamma}}{4} z + f_0 + \frac{f_1}{z} + \ldots, \qquad g'(z) \sim -\frac{\mathrm{i}\dot{\gamma}}{2} z + g_0 + \frac{g_1}{z} + \ldots \tag{11}$$

as $|z| \to \infty$ where f_0 and g_0 satisfy

$$-\overline{f_0} + g_0 = 0 \tag{12}$$

in order that the uniform flow component in the far-field vanishes. We emphasize again that coefficients such as f_0 and g_0 will be functions of time even if our notation does not make this feature explicit.

An advantage of the complex variable formulation of Stokes flow is that the condition

of zero total force on the fiber takes a form that is particularly easy to enforce. From the complex form of the stress tensor (8) as an exact derivative with respect to arclength s, one sees that the net force on the fiber is related to the change of the quantity $H(z, \overline{z})$ on making a closed circuit around the fiber. The condition that the latter is free of any net force therefore requires that $f(z)$ and $g'(z)$ are *single-valued* functions on encircling the fiber. Furthermore, if the fiber is force-free the condition that the fiber is *also* free of net torque can be shown to be equivalent to

$$\mathrm{Im}[g_1] = 0. \tag{13}$$

The incompressibility of the fluid, and the fact that there are no other sources or sinks in the fluid, implies that

$$\mathrm{Re}[g_1] = 0 \tag{14}$$

which allows us to conclude that, for our problem, $g_1 = 0$. The value of f_1, and all higher coefficients in the far-field expansions (11), are then determined by the solution.

Any fiber, straight or curved, of vanishing thickness will have a corner of angle 2π at its end-points. It is well-known in low-Reynolds-number hydrodynamics[20,21,23] that one must expect the presence of singularities in the physical quantities, and hence also of $f(z)$ and $g(z)$, at any such corner points. A local analysis shows that both $f(z)$ and $g(z)$ exhibit square root singularities at the end-points of the fiber; the fluid velocity is finite and the fluid stress has integrable singularities at these points. Apart from these square root singularities, and the simple poles (11) at infinity forced by the background shear, $f(z)$ and $g(z)$ must be analytic functions in the fluid region.

The use of the methods of complex analysis for two-dimensional Stokes flows is rare compared to plane elasticity where similar boundary value problems for biharmonic fields arise[22]; the role of the fluid velocity components in Stokes flow are analogous to the displacement components in a plane elastic medium. In linear elasticity, however, it is usual to assume that displacements are small but any such restriction on the velocities for the fiber evolution problem considered here is clearly not appropriate.

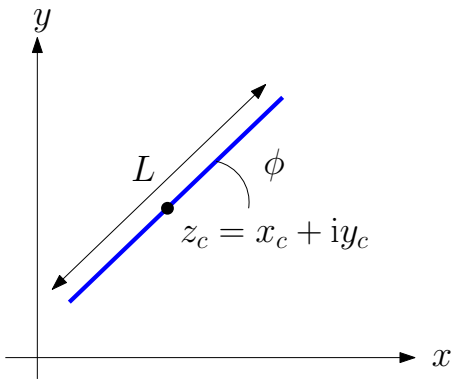


FIG. 2. Straight fiber of length L centred at the origin with orientation ϕ.

III. STRAIGHT FIBERS

Before proceeding to the curved fiber analysis it is instructive to first derive the evolution equation for a straight rigid fiber in a linear shear; the straight fiber analysis is comparatively simple and will prepare the reader for the more involved treatment of §IV needed for curved fibers. Of course, the curved fiber analysis of §IV retrieves the straight fiber result in an appropriate limit, but the separate analysis in this section offers a more direct approach. Moreover, the following derivation of the governing ordinary differential equations via the methods of complex analysis and use of the Joukowski conformal mapping[27] (more familiar to fluid dynamicists in ideal inviscid flow scenarios) appears to be new and worth documenting.

Consider a straight rigid fiber that is free of both force and torque situated in the simple shear (10). Let z_c denote its midpoint location as shown in Figure 2. To make progress, we will employ some conformal mapping techniques. The Joukowski conformal mapping[27] from the interior of a unit ζ-disc in a complex ζ-plane to the region exterior to a straight fiber of length $L = 4R$ and orientation ϕ to the positive real axis is

$$z = z(\zeta) = z_c + Re^{\mathrm{i}\phi}\left[\frac{1}{\zeta} + \zeta\right]. \tag{15}$$

Here, and throughout, as seen in (15) we abuse notation in using z to refer both to the complex coordinate in the physical plane *and* the conformal mapping function, but there should be no confusion in doing so.

Under the mapping (15) the points $\zeta = \pm 1$ are transplanted to the end-points of the

fiber; clearly, $\zeta = 0$ is the preimage of $z = \infty$. Since

$$z - z_c = re^{\mathrm{i}\phi}, \qquad \overline{z} - \overline{z_c} = re^{-\mathrm{i}\phi} \tag{16}$$

then

$$\overline{z} - \overline{z_c} = e^{-2\mathrm{i}\phi}(z - z_c). \tag{17}$$

It is helpful to introduce the Schwarz function[28] $\mathcal{S}(z)$ of the fiber defined as the function, analytic in an annular neighbourhood containing the fiber, satisfying

$$\mathcal{S}(z) = \overline{z} \tag{18}$$

on it. From (17) the Schwarz function $\mathcal{S}(z)$ of the straight fiber is seen to be

$$\mathcal{S}(z) = \overline{z_c} + e^{-2\mathrm{i}\phi}(z - z_c). \tag{19}$$

The boundary condition on the fiber is conveniently written as

$$u - \mathrm{i}v = \overline{U} - \mathrm{i}\Omega(\overline{z} - \overline{z_c}), \tag{20}$$

where the complex-valued fiber velocity $U \in \mathbb{C}$ and its angular velocity $\Omega \in \mathbb{R}$ are to be found. The latter two quantities will follow from the requirements that the fiber is free of net force and torque. On use of the (conjugate of the) second relation in (5) we can write

$$-\overline{f(z)} + \overline{z}f'(z) + g'(z) = \overline{U} - \mathrm{i}\Omega(\overline{z} - \overline{z_c}) \tag{21}$$

and this, together with the conditions at infinity and at the end-points of the fiber, will determine $f(z)$ and $g(z)$.

In fact, our approach will be to determine the composed functions defined to be

$$F(\zeta) \equiv f(z(\zeta)), \qquad G(\zeta) \equiv g'(z(\zeta)) \tag{22}$$

(21) implies that, on the fiber,

$$g'(z(\zeta)) = G(\zeta) = \overline{U} - \mathrm{i}\Omega(\mathcal{S}(z) - \overline{z_c}) - \mathcal{S}(z)f'(z) + \overline{F}(1/\zeta), \tag{23}$$

where we have used the fact that $\overline{\zeta} = 1/\zeta$ on the fiber and the Schwarz conjugate function $\overline{F}(\zeta)$ to $F(\zeta)$ (and any other analytic function) defined by $\overline{F}(\zeta) \equiv \overline{F(\overline{\zeta})}$. Since (23) now relates analytic functions, it can be analytically continued *off* the fiber.

The far-field conditions (11) imply the leading order behaviour

$$F(\zeta) \sim \frac{\mathrm{i}\dot{\gamma}Re^{\mathrm{i}\phi}}{4\zeta}, \qquad G(\zeta) \sim -\frac{\mathrm{i}\dot{\gamma}Re^{\mathrm{i}\phi}}{2\zeta}, \qquad \text{as } \zeta \to 0. \tag{24}$$

The functions $F(\zeta)$ and $G(\zeta)$ must also be single-valued in the unit ζ-disc to ensure the fiber is force-free. The condition of zero net torque is (13).

We will now demonstrate that the solution for $F(\zeta)$ has the rational function form

$$F(\zeta) = \frac{A}{\zeta} + B\zeta \tag{25}$$

for suitable A and B which change in time as the fiber evolves. We might have added another constant term to (25), but setting it to zero fixes an aforementioned additive degree of freedom in specifying $f(z)$. To satisfy (24) we need

$$A = \frac{\mathrm{i}\dot{\gamma}Re^{\mathrm{i}\phi}}{4}, \tag{26}$$

where we have used that fact that $z \sim Re^{\mathrm{i}\phi}/\zeta$ as $\zeta \to 0$ or $z \to \infty$.

By the chain rule, and by a Taylor expansion, we find

$$f'(z) = \frac{F'(\zeta)}{z'(\zeta)} = \frac{1}{Re^{\mathrm{i}\phi}}\frac{A - B\zeta^2}{1 - \zeta^2} = \frac{1}{Re^{\mathrm{i}\phi}}\left[A + (A - B)\zeta^2 + \mathcal{O}(\zeta^4)\right]. \tag{27}$$

Also,

$$\overline{F}(1/\zeta) = \overline{A}\zeta + \frac{\overline{B}}{\zeta} = \overline{B}\left(\zeta + \frac{1}{\zeta}\right) + (\overline{A} - \overline{B})\zeta = \frac{\overline{B}z}{Re^{\mathrm{i}\phi}} + (\overline{A} - \overline{B})\zeta, \tag{28}$$

where we have used the fact that

$$\left[\frac{1}{\zeta}+\zeta\right]=\frac{z}{Re^{\mathrm{i}\phi}}. \tag{29}$$

Making use of all this in (23) implies that, as $z\to\infty$,

$$\begin{aligned} g'(z)\sim{}&\overline{U}-\mathrm{i}\Omega e^{-2\mathrm{i}\phi}(z-z_c)-(\overline{z_c}+e^{-2\mathrm{i}\phi}(z-z_c))\left[\frac{\mathrm{i}\dot{\gamma}}{4}+\frac{(A-B)}{Re^{\mathrm{i}\phi}}\zeta^2+\mathcal{O}(\zeta^4)\right]\\ &+\frac{\overline{B}z}{Re^{\mathrm{i}\phi}}+(\overline{A}-\overline{B})\zeta \end{aligned} \tag{30}$$

or, since $\zeta\sim Re^{\mathrm{i}\phi}/z$ as $z\to\infty$,

$$\begin{aligned} g'(z)\sim{}&\overline{U}-\mathrm{i}\Omega e^{-2\mathrm{i}\phi}(z-z_c)-(\overline{z_c}+e^{-2\mathrm{i}\phi}(z-z_c))\left[\frac{\mathrm{i}\dot{\gamma}}{4}+\frac{(A-B)Re^{\mathrm{i}\phi}}{z^2}+\mathcal{O}(1/z^4)\right]\\ &+\frac{\overline{B}z}{Re^{\mathrm{i}\phi}}+(\overline{A}-\overline{B})\frac{Re^{\mathrm{i}\phi}}{z}+\mathcal{O}(1/z^2) \end{aligned} \tag{31}$$

The far-field boundary condition (24) on $G(\zeta)$ implies that

$$-\mathrm{i}\Omega e^{-2\mathrm{i}\phi}-\frac{\mathrm{i}\dot{\gamma}e^{2\mathrm{i}\phi}}{4}+\frac{\overline{B}}{Re^{\mathrm{i}\phi}}=-\frac{\mathrm{i}\dot{\gamma}}{2},\qquad\text{or}\qquad B=-\mathrm{i}\Omega Re^{\mathrm{i}\phi}-\frac{\mathrm{i}\dot{\gamma}Re^{\mathrm{i}\phi}}{4}+\frac{\mathrm{i}\dot{\gamma}Re^{-\mathrm{i}\phi}}{2}. \tag{32}$$

Then

$$g'(z)\sim-\frac{\mathrm{i}\dot{\gamma}z}{2}+g_0+\ldots\qquad\text{where}\qquad g_0=\overline{U}+\mathrm{i}\Omega e^{-2\mathrm{i}\phi}z_c-\frac{\mathrm{i}\dot{\gamma}}{4}\left(\overline{z_c}-e^{-2\mathrm{i}\phi}z_c\right)-\frac{\overline{B}z_c}{Re^{\mathrm{i}\phi}}. \tag{33}$$

But we also know that

$$F(\zeta)\sim\frac{\mathrm{i}\dot{\gamma}z}{4}+f_0+\ldots\qquad\text{with}\qquad f_0=-\frac{Az_c}{Re^{\mathrm{i}\phi}} \tag{34}$$

so condition (12) implies, after simplification and substitution for A and B from (26) and (32), that

$$U=\dot{\gamma}y_c. \tag{35}$$

Finally, extraction of the $1/z$ coefficient of $g'(z)$ in (31) shows that imposing the torque-free condition requires that

$$\mathrm{Im}\left[(A-B)e^{-\mathrm{i}\phi}\right]=0. \tag{36}$$

From (26) and (32) we find

$$(A-B)e^{-\mathrm{i}\phi} = \mathrm{i}\Omega R - \frac{\mathrm{i}\dot{\gamma}Re^{-2\mathrm{i}\phi}}{2} + \frac{\mathrm{i}\dot{\gamma}R}{2}. \tag{37}$$

Hence the torque-free condition (36) leads to

$$\Omega = -\frac{\dot{\gamma}}{2} + \frac{\dot{\gamma}}{2}\cos 2\phi = -\dot{\gamma}\sin^2\phi. \tag{38}$$

The final system of ordinary differential equations is

$$\frac{dx_c}{dt} = \dot{\gamma}y_c, \qquad \frac{dy_c}{dt} = 0, \qquad \frac{d\phi}{dt} = -\dot{\gamma}\sin^2\phi. \tag{39}$$

It is interesting to observe that the same equations govern the evolution of a 3D fiber in simple shear – a fact derivable as a limit of the Jeffery equations[1] for a rigid ellipsoid, or by an exercise in slender-body theory. It is on the basis of this fact that we anticipate that the dynamical system to be derived next for a *curved* 2D fiber will also be relevant to a slender 3D fiber when it evolves in the plane of the shear.

We conclude this section by discussing the square root singularities of $f(z)$ and $g(z)$ which, from earlier commentary, are expected at the end-points of the fiber; the analysis just given appears not to have involved any such square roots. But these have been incorporated into the solution by virtue of our very mathematical approach via conformal mapping. To see this, the inverse conformal mapping function denoted by $\zeta = \zeta(z)$ is

$$\zeta = \zeta(z) = \frac{\mathcal{Z} - [\mathcal{Z}^2 - 4]^{1/2}}{2}, \qquad \mathcal{Z} \equiv \frac{z - z_c}{Re^{\mathrm{i}\phi}}, \tag{40}$$

which can be seen to have square root singularities at the fiber end-points. Hence on rewriting the rational function solutions for $F(\zeta)$ and $G(\zeta)$ in terms of z by substituting for $\zeta = \zeta(z)$ from (40) the presence of the expected square root singularities becomes apparent.

This feature of having the requisite square root singularities "built in" is one of the advantages of our mathematical approach. Other possible methods, such as generalizing Hasimoto's approach[23] to flows through gaps in a wall, usually require explicit consideration of those end-point singularities. Crowdy & Samson[3] have previously applied variants of the conformal mapping approach advocated here to the various Stokes flow problems considered

by Hasimoto[23], Smith[24] and Ko & Jeong[25].

IV. CURVED FIBERS IN SIMPLE SHEAR

The idea now is to generalize the previous construction to curved fibers. Consider a curved fiber with midpoint at

$$z_c = x_c + \mathrm{i}y_c \tag{41}$$

and making angle ϕ with the positive x-axis as shown in Figure 1. We suppose it has length L and radius of curvature R. Since the fiber is a rigid body the latter quantities are fixed in time and it is only necessary to track the evolution of z_c and ϕ.

To extend the analysis of §III we need the relevant generalization of the classical Joukowski mapping to a curved fiber. Such a mapping, which is another example of a so-called conformal slit mapping[27], has been employed by the author in a study of two-dimensional Janus particles[29] and we can put it to use again here. The only previous study of two-dimensional Stokes flow involving circular arcs that we have been able to find in the literature is that of Hasimoto[26] who studied the formation of recirculating Moffatt-type eddies in flows past circular-arc airfoils in fixed position.

Let

$$z(\zeta) = z_c - \mathrm{i}e^{\mathrm{i}\phi}R\left[1 + \eta(\zeta)\right], \tag{42}$$

where

$$\eta(\zeta) = \frac{(\zeta - \overline{\alpha})(\zeta - 1/\overline{\alpha})}{(\zeta - \alpha)(\zeta - 1/\alpha)}, \qquad \alpha = \mathrm{i}r, \qquad 0 < r < 1. \tag{43}$$

For $0 < r < 1$ the subsidiary conformal mapping (43) transplants the unit ζ-disc to the exterior to the circular-arc slit, in a complex η-plane, along the unit η-circle subtending angles $[\pi - \beta, \pi + \beta]$ at the origin (where $0 < \beta < \pi$); the point $\zeta = \alpha$ maps to $\eta = \infty$. Figure 3 shows a schematic. In the η-plane the fiber has length $2(\pi - \beta)$ where[29]

$$r = \tan\left(\frac{\pi - \beta}{4}\right). \tag{44}$$

Consequently, with the simple change of origin, rescaling and rotation effected in (42) the conformal mapping $z = z(\zeta)$ transplants the same unit ζ-disc to a curved fiber in the physical

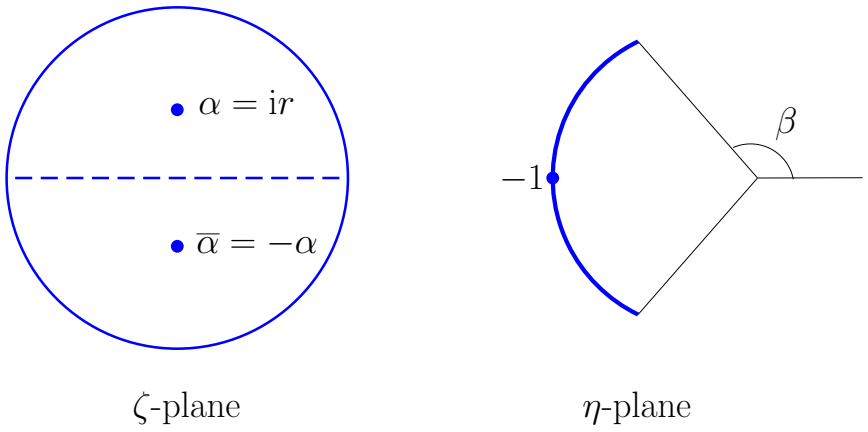


FIG. 3. The mapping $\eta(\zeta)$ given in (43) transplants the interior of the unit ζ-disc to the exterior of a circular-arc segment of the unit η-circle $\arg[\eta] \in [\pi - \beta, \pi + \beta]$. The point $\zeta = \alpha = \mathrm{i}r$ with $0 < r < 1$ maps to $\eta = \infty$ with r and β related via (44).

z-plane with midpoint at z_c, orientation ϕ, radius of curvature R and length

$$L = 2(\pi - \beta)R. \tag{45}$$

This is exactly the required fiber geometry shown in Figure 1. The point $\zeta = \alpha$ is the preimage of $z = \infty$.

As before the Schwarz function of the curved fiber, again denoted by $\mathcal{S}(z)$, is useful. Suppose the fiber lies on the circle

$$|z - c|^2 = R^2, \qquad \text{where} \qquad c = z_c - \mathrm{i}Re^{\mathrm{i}\phi} \tag{46}$$

is center of the circle on which the curved fiber lies; the expression for c in terms of z_c can be derived from elementary geometrical considerations in the z-plane. Then

$$\mathcal{S}(z) = \overline{c} + \frac{R^2}{z - c} = \overline{z_c} + \mathrm{i}Re^{-\mathrm{i}\phi} + \frac{R^2}{z - c}. \tag{47}$$

The partial fraction decomposition

$$\frac{(\zeta - \overline{\alpha})(\zeta - 1/\overline{\alpha})}{\zeta - 1/\alpha} = \zeta + \left[\alpha + \frac{2}{\alpha}\right] + 2\left(1 + \frac{1}{\alpha^2}\right)\frac{1}{\zeta - 1/\alpha} \tag{48}$$

is helpful in facilitating the calculation of the Laurent expansion

$$z = \frac{Q}{\zeta - \alpha} + P + S(\zeta - \alpha) + \mathcal{O}((\zeta - \alpha)^2) \tag{49}$$

about the point $\zeta = \alpha$ where

$$Q = -2rRe^{\mathrm{i}\phi}\left(\frac{1-r^2}{1+r^2}\right), \qquad P = z_c - \mathrm{i}Re^{\mathrm{i}\phi}\left[2 - \frac{2(1-r^2)}{(1+r^2)^2}\right], \qquad S = \frac{Q}{(1+r^2)^2}. \tag{50}$$

It can then be established that, as $\zeta \to \alpha$,

$$\frac{1}{\zeta - \alpha} = \frac{z}{Q} - \frac{P}{Q} - \frac{S}{z} + \mathcal{O}(1/z^2), \qquad (\zeta - \alpha) = \frac{Q}{z} + \mathcal{O}(1/z^2). \tag{51}$$

After these mathematical preliminaries we proceed to study the governing boundary value problem for the fiber's motion in simple shear. The boundary condition on the rigid fiber is again

$$u - \mathrm{i}v = -\overline{f(z)} + \overline{z}f'(z) + g'(z) = \overline{U} - \mathrm{i}\Omega(\overline{z} - \overline{z_c}), \tag{52}$$

where U and Ω are to be determined. The same functions $F(\zeta)$ and $G(\zeta)$ introduced in (22) are useful. The far-field conditions (11) on these Goursat functions still pertain.

Condition (52) can be written in the form

$$-\overline{F}(1/\zeta) + \mathcal{S}(z)f'(z) + G(\zeta) = \overline{U} - \mathrm{i}\Omega(\mathcal{S}(z) - \overline{z_c}). \tag{53}$$

By analytic continuation off the fiber we find the following expression for $G(\zeta)$ in terms of $F(\zeta)$, its Schwarz conjugate, and the Schwarz function $\mathcal{S}(z)$:

$$G(\zeta) = \overline{F}(1/\zeta) - \mathcal{S}(z)f'(z) + \overline{U} - \mathrm{i}\Omega(\mathcal{S}(z) - \overline{z_c}), \tag{54}$$

which turns out to be convenient for studying the far-field behaviour.

We now show that the exact solution for $F(\zeta)$ is given by the rational function

$$F(\zeta) = \frac{A}{\zeta - \alpha} + \frac{B}{1/\zeta - \overline{\alpha}} + \frac{C}{1/\zeta - \alpha}, \tag{55}$$

for A, B and C to be determined; the parameters are functions of time only and depend on

the instantaneous fiber configuration. The equation

$$A = \frac{\mathrm{i}\dot{\gamma}Q}{4} = -\frac{\mathrm{i}e^{\mathrm{i}\phi}r\dot{\gamma}R}{2}\left[\frac{1-r^2}{1+r^2}\right] \tag{56}$$

is forced by the requirement that $f(z)$ has the leading order far-field behaviour given in (11). It remains to find B and C.

Clearly

$$\overline{F}(1/\zeta) = \frac{\overline{A}}{1/\zeta - \overline{\alpha}} + \frac{\overline{B}}{\zeta - \alpha} + \frac{\overline{C}}{\zeta - \overline{\alpha}} \tag{57}$$

from which we deduce the following Laurent expansion about $\zeta = \alpha$:

$$\overline{F}(1/\zeta) \sim \frac{\overline{B}}{\zeta - \alpha} + \left[\frac{\overline{C}}{2\alpha} + \frac{\overline{A}\alpha}{1-|\alpha|^2}\right] + (\zeta - \alpha)\left[-\frac{\overline{C}}{4\alpha^2} + \frac{\overline{A}}{(1-|\alpha|^2)^2}\right] + \mathcal{O}((\zeta-\alpha)^2). \tag{58}$$

Hence on use of (51) we find, as $z \to \infty$,

$$\overline{F}(1/\zeta) \sim \overline{B}\left[\frac{z}{Q} - \frac{P}{Q} - \frac{S}{z}\right] + \left[\frac{\overline{C}}{2\alpha} + \frac{\overline{A}\alpha}{1-|\alpha|^2}\right] + \left[\frac{\overline{A}}{(1-|\alpha|^2)^2} - \frac{\overline{C}}{4\alpha^2}\right]\frac{Q}{z} + \mathcal{O}(1/z^2). \tag{59}$$

We also know, from (47) and the far-field condition (11), that as $z \to \infty$,

$$\mathcal{S}(z) \sim \overline{z_c} + \mathrm{i}e^{-\mathrm{i}\phi}R + \frac{R^2}{z} + \mathcal{O}(1/z^2), \qquad f'(z) \sim \frac{\mathrm{i}\dot{\gamma}}{4} + \mathcal{O}(1/z^2). \tag{60}$$

On substitution of (59) and (60) into (54) we find

$$\begin{aligned} G(\zeta) = {} & \overline{B}\left[\frac{z}{Q} - \frac{P}{Q} - \frac{S}{z}\right] + \left[\frac{\overline{C}}{2\alpha} + \frac{\overline{A}\alpha}{1-|\alpha|^2}\right] + \left[\frac{\overline{A}}{(1-|\alpha|^2)^2} - \frac{\overline{C}}{4\alpha^2}\right]\frac{Q}{z} \\ & - \frac{\mathrm{i}\dot{\gamma}}{4}\left[\overline{z_c} + \mathrm{i}Re^{-\mathrm{i}\phi} + \frac{R^2}{z}\right] + \overline{U} - \mathrm{i}\Omega\left(\mathrm{i}Re^{-\mathrm{i}\phi} + \frac{R^2}{z}\right) + \mathcal{O}(1/z^2), \end{aligned} \tag{61}$$

as $|z| \to \infty$. Examination of the coefficient of z yields

$$\frac{\overline{B}}{Q} = -\frac{\mathrm{i}\dot{\gamma}}{2}, \quad \text{or} \quad B = -2\overline{A} = \mathrm{i}e^{-\mathrm{i}\phi}r\dot{\gamma}R\left[\frac{1-r^2}{1+r^2}\right] \tag{62}$$

in order that $g'(z)$ has the required far-field behaviour (11). This determines B.

If the fiber is to be free of torque we must enforce the condition that the $\mathcal{O}(1/z)$ term in

the far-field expansion (61) of $g'(z)$ vanishes, i.e.,

$$-\overline{B}S + Q\left[\frac{\overline{A}}{(1-|\alpha|^2)^2} - \frac{\overline{C}}{4\alpha^2}\right] - \frac{\mathrm{i}\dot{\gamma}R^2}{4} - \mathrm{i}\Omega R^2 = 0 \tag{63}$$

or, equivalently,

$$\mathrm{i}\Omega = -\frac{\mathrm{i}\dot{\gamma}}{4} - \frac{\overline{B}S}{R^2} + \frac{Q}{R^2}\left[\frac{\overline{A}}{(1-r^2)^2} + \frac{\overline{C}}{4r^2}\right]. \tag{64}$$

The real part of (64) can be shown, after some algebra, to imply

$$\mathrm{Re}[e^{\mathrm{i}\phi}\overline{C}] = \frac{2\mathrm{i}R\dot{\gamma}r^3(1-r^2)}{(1+r^2)^3}[e^{2\mathrm{i}\phi} - e^{-2\mathrm{i}\phi}]. \tag{65}$$

Next observe from (57) that $\overline{F}(1/\zeta)$ has a simple pole at $\zeta = \overline{\alpha}$ which is inside the unit ζ-disc; $\overline{z}(1/\zeta)$ has a simple pole there too. Another form of (54) is

$$G(\zeta) = \overline{F}(1/\zeta) - \overline{z}(1/\zeta)\frac{F'(\zeta)}{z'(\zeta)} + \overline{U} - \mathrm{i}\Omega(\overline{z}(1/\zeta) - \overline{z_c}) \tag{66}$$

from which it is clear that $G(\zeta)$ will have an unwanted simple pole at $\zeta = \overline{\alpha}$ – produced by the term $\overline{F}(1/\zeta)$ as well as those involving $\overline{z}(1/\zeta)$ – unless it is removed. After some algebra the condition that $\zeta = \overline{\alpha}$ is a *removable* singularity of $G(\zeta)$ is found to be

$$\mathrm{Im}[e^{\mathrm{i}\phi}\overline{C}] = \frac{R\dot{\gamma}r}{2}\left(\frac{1-r^2}{1+r^2}\right)\left[1 - \left(\frac{1-r^2}{1+r^2}\right)^2(e^{2\mathrm{i}\phi} + e^{-2\mathrm{i}\phi})\right]. \tag{67}$$

A combination of (65) and (67) give an expression for $e^{\mathrm{i}\phi}\overline{C}$ from which we deduce

$$\overline{C} = \frac{2\mathrm{i}R\dot{\gamma}r^3(1-r^2)}{(1+r^2)^3}[e^{\mathrm{i}\phi} - e^{-3\mathrm{i}\phi}] + \frac{\mathrm{i}R\dot{\gamma}r}{2}\left(\frac{1-r^2}{1+r^2}\right)\left[e^{-\mathrm{i}\phi} - \left(\frac{1-r^2}{1+r^2}\right)^2(e^{\mathrm{i}\phi} + e^{-3\mathrm{i}\phi})\right] \tag{68}$$

which (on complex conjugation) determines C. In this way, since A, B and C are determined then so is $F(\zeta)$.

The function $G(\zeta)$ will follow from (66) once Ω and U have been found. But on substitution of (56), (62) and (68) into (64) it follows, after some algebra, that

$$\Omega = -\frac{\dot{\gamma}}{2} + \frac{\dot{\gamma}}{2}\left(\frac{1-r^2}{1+r^2}\right)^2\cos 2\phi = -\frac{\dot{\gamma}}{2} + \frac{\dot{\gamma}}{2}\cos^2\left[\frac{L}{4R}\right]\cos 2\phi, \tag{69}$$

where we have also used (44), (45) and some trigonometric identities.

The only thing left is to find U, and this follows by enforcing (12). From (55) and (51), as $|z| \to \infty$,

$$F(\zeta) = A\left[\frac{z}{Q} - \frac{P}{Q}\right] + \frac{B}{1/\alpha - \overline{\alpha}} + \frac{C}{1/\alpha - \alpha} + \mathcal{O}(1/z) = \frac{\mathrm{i}\dot{\gamma}z}{4} + f_0 + \mathcal{O}(1/z), \tag{70}$$

where

$$f_0 = -\frac{\mathrm{i}\dot{\gamma}P}{4} + \frac{\mathrm{i}Br}{1-r^2} + \frac{\mathrm{i}Cr}{1+r^2}. \tag{71}$$

On the other hand, from (61), we identify

$$g_0 = -\frac{\overline{B}P}{Q} + \left[\frac{\overline{C}}{2\alpha} + \frac{\overline{A}\alpha}{1-|\alpha|^2}\right] - \frac{\mathrm{i}\dot{\gamma}}{4}\left[\overline{z_c} + \mathrm{i}Re^{-\mathrm{i}\phi}\right] + \overline{U} + \Omega R e^{-\mathrm{i}\phi}. \tag{72}$$

Hence (12) leads, after some algebra, to

$$\overline{U} = \frac{\mathrm{i}\dot{\gamma}}{4}(\overline{P} - 2P + \overline{z_c} + \mathrm{i}Re^{-\mathrm{i}\phi}) + \frac{r^2 R\dot{\gamma}}{2(1+r^2)}(2e^{\mathrm{i}\phi} + e^{-\mathrm{i}\phi}) + \frac{\mathrm{i}\overline{C}}{2r}\frac{1-r^2}{1+r^2} - \Omega R e^{-\mathrm{i}\phi}, \tag{73}$$

where we have substituted for A and B from (56) and (62). But

$$\overline{P} + \overline{z_c} - 2P = 2(\overline{z_c} - z_c) + 2\mathrm{i}R\left[1 - \frac{1-r^2}{(1+r^2)^2}\right](2e^{\mathrm{i}\phi} + e^{-\mathrm{i}\phi}) \tag{74}$$

yielding, on substitution into (73),

$$\overline{U} = \frac{\dot{\gamma}(z_c - \overline{z_c})}{2\mathrm{i}} - \frac{R\dot{\gamma}e^{-\mathrm{i}\phi}}{4} - \frac{\dot{\gamma}Rr^2}{(1+r^2)^2}(2e^{\mathrm{i}\phi} + e^{-\mathrm{i}\phi}) + \frac{\mathrm{i}\overline{C}}{2r}\frac{1-r^2}{1+r^2} - \Omega R e^{-\mathrm{i}\phi}. \tag{75}$$

On substituting for $\overline{C}$ from (68), and for Ω from (69), further algebraic manipulations and use of trigonometric identities yields

$$U = \dot{\gamma}y_c - \frac{\dot{\gamma}R}{2}\left[1 - \cos^4\left(\frac{L}{4R}\right)\right]e^{-\mathrm{i}\phi}. \tag{76}$$

Finally the relations

$$\frac{dz_c}{dt} = U, \qquad \frac{d\phi}{dt} = \Omega \tag{77}$$

produce the dynamical system (1) on equating real and imaginary parts.

A valuable check on the analysis is provided by the two limiting cases $L/R \to 0$ and $L/R \to 2\pi$. As $L/R \to 0$ we retrieve the result (39) for the straight fiber. In the limit, $L/R \to 2\pi$, where the two ends of the circular fiber close up to form the entire boundary of a circular disc, we find

$$\frac{dz_c}{dt} \to \dot{\gamma} y_c - \frac{\dot{\gamma} R}{2} e^{-\mathrm{i}\phi}. \qquad \frac{d\phi}{dt} \to -\frac{\dot{\gamma}}{2}. \tag{78}$$

But on differentiation of the expression (46) for c, and use of (78), we find

$$\frac{dc}{dt} = \frac{dz_c}{dt} + R\frac{d\phi}{dt} e^{\mathrm{i}\phi} = \frac{dz_c}{dt} - \frac{\dot{\gamma} R}{2} e^{\mathrm{i}\phi} = \dot{\gamma} y_c - \frac{\dot{\gamma} R}{2} e^{-\mathrm{i}\phi} - \frac{\dot{\gamma} R}{2} e^{\mathrm{i}\phi} = \dot{\gamma}\mathrm{Im}[c]. \tag{79}$$

In this way we retrieve the system

$$\frac{dc}{dt} = \dot{\gamma}\mathrm{Im}[c], \qquad \frac{d\phi}{dt} \to -\frac{\dot{\gamma}}{2} \tag{80}$$

which is easily shown to constitute the evolution equations for a circular disc in simple shear.

While the derivation of this dynamical system has been our primary goal it is worth remembering that, in determining A, B, C, U and Ω, we have simultaneously solved for the full ambient Stokes flow by determining the form of the two Goursat functions

$$\begin{aligned} F(\zeta) &= \frac{A}{\zeta - \alpha} + \frac{B}{1/\zeta - \overline{\alpha}} + \frac{C}{1/\zeta - \alpha}, \\ G(\zeta) &= \overline{F}(1/\zeta) - \overline{z}(1/\zeta)\frac{F'(\zeta)}{z'(\zeta)} + \overline{U} - \mathrm{i}\Omega(\overline{z}(1/\zeta) - \overline{z_c}) \end{aligned} \tag{81}$$

from which all physical quantities such as velocities and pressures can be extracted if needed. Indeed, the complex velocity field is given in terms of $(\zeta, \overline{\zeta})$ by

$$u - \mathrm{i}v = \overline{F}(1/\zeta) - \overline{F(\zeta)} + \frac{F'(\zeta)}{z'(\zeta)}\left[\overline{z(\zeta)} - \overline{z}(1/\zeta)\right] + \overline{U} - \mathrm{i}\Omega\left[\overline{z}(1/\zeta) - \overline{z_c}\right]. \tag{82}$$

V. FIBER DYNAMICS IN SIMPLE SHEAR

We now study the dynamics of system (1). Henceforth we set $\dot{\gamma} = 1$ which is equivalent to nondimensionalizing time using the shear rate. Since the right hand side of (1) is independent of x_c the dynamical system is integrable and, in principle, an understanding of the dynamics

can be reduced to a study of the (ϕ, y_c) phase portrait of the ordinary differential equation

$$\frac{dy_c}{d\phi} = R\left[1 - \cos^4\left(\frac{L}{4R}\right)\right] \frac{\sin\phi}{\left\{-1 + \cos^2\left(\frac{L}{4R}\right)\cos 2\phi\right\}}. \tag{83}$$

This is a first-order, separable, nonlinear ordinary differential equation which can be integrated explicitly. But a display of the mathematical formulas for the integral curves is not illuminating and, instead, we study (1) by direct numerical integration of the full system.

The dynamics is found to depend sensitively on the geometry of the fiber but only through the quantity $\cos(L/4R)$. One sees immediately from (1) that the curvature of the fiber will produce more complicated dynamics than a straight fiber: in the straight fiber limit $R \to \infty$ then $\cos(L/4R) \to 1$ and the equation for $\dot{z}_c$ reduces to that given by (35), i.e.,

$$\frac{dx_c}{dt} = \dot{\gamma} y_c, \qquad \frac{dy_c}{dt} = 0, \tag{84}$$

meaning, for example, that any fiber with centre located initially on $y = 0$ will remain stationary and will simply reorient about its centroid with angular velocity given by (38). But as soon as the fiber becomes even slightly curved this is no longer possible and the equations for $\dot{x}_c$ and $\dot{y}_c$ each acquire a new term proportional to

$$\left[1 - \cos^4\left(\frac{L}{4R}\right)\right] \tag{85}$$

meaning that even slightly curved fibers are inclined to translate both in and across the streamwise direction.

For curved fibers generic motions for any initial condition are found to be translating periodic orbits with a net streamwise displacement during each nondimensional period

$$T = \frac{4\pi}{\sqrt{1 - \cos^4\left(\frac{L}{4R}\right)}}. \tag{86}$$

Figure 4 shows a graph of T against $\cos(L/4R)$. When $R \to \infty$, so that the fiber becomes straight, the period of the orbit tends to infinity. This is as expected given that a straight rigid fiber is known to simply align itself with the flow without rotating in any periodic

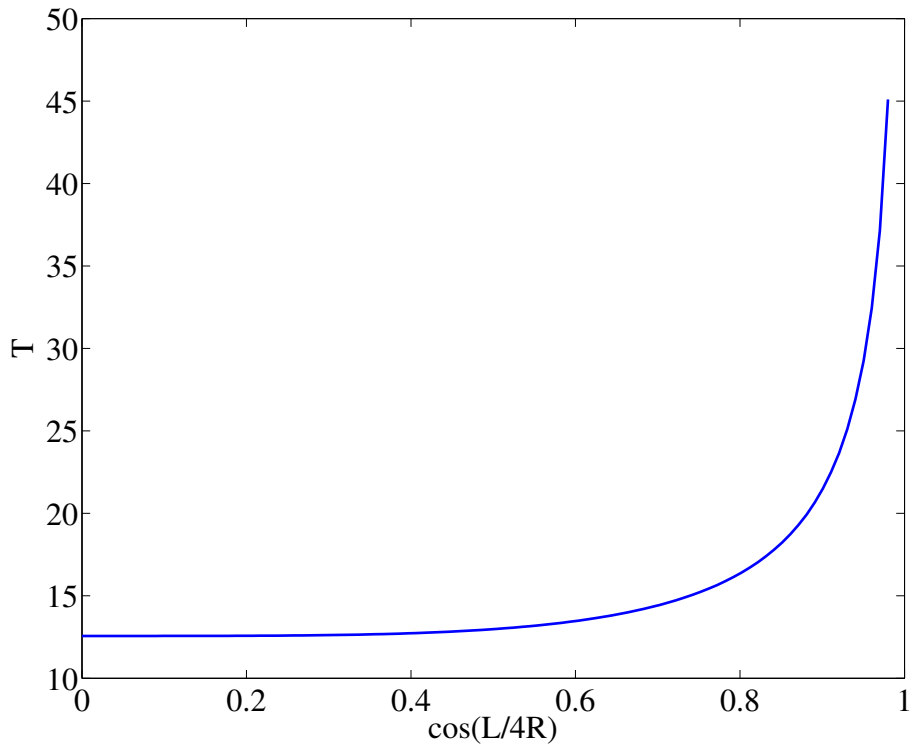


FIG. 4. Orbital period T as a function of $\cos(L/4R)$.

fashion.

Slightly curved fibers exhibit trajectories with the same characteristic behaviour identified in[15] whereby the fiber moves in such a way as to "scoop" up the oncoming shear flow until it is largely perpendicular to the stream and then rapidly "flip" spending only short periods perpendicular to the stream, before returning to its original orientation now displaced by some distance in the flow direction. Figure 5 shows typical trajectories over a single period for various values of $\cos(L/4R)$. The degree of scoop, and the duration of the flip, vary significantly with $\cos(L/4R)$. Figure 6 shows the time evolution of the orientation $\phi(t)$, over a single period, for typical orbits labelled by their values of $\cos(L/4R)$. A step-like structure of this graph, most prevalent for $\cos(L/4R)$ close to unity (nearly straight, or weakly curved, fibers), is indicative of a rapid flipping motion; a steep vertical slope of this graph means that the fiber orientation changes dramatically over a short time period. As $\cos(L/4R) \to 0$ this tendency to flip gradually disappears and the angular velocity "smooths out" to the constant value $-1/2$.

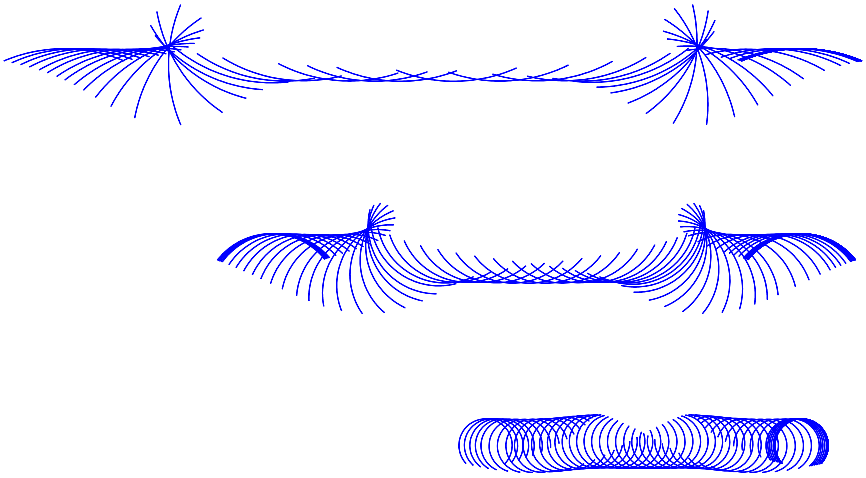


FIG. 5. "Flip-scoop" trajectories for different curved fibers: $L = 1$ with $z_c(0) = 0, \phi(0) = 0$ and $\cos(L/4R) = 0.98$ (top), 0.9 (middle) and 0.4 (bottom).

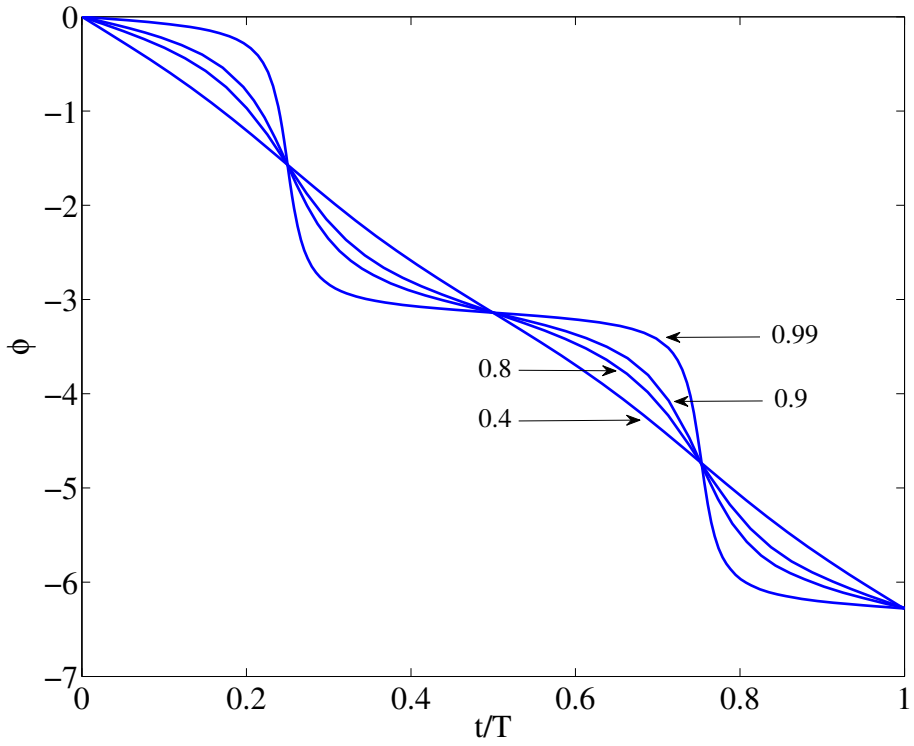


FIG. 6. The degree of "flip": graphs of $\phi(t)$ against t/T with orbits labelled by $\cos(L/4R)$. A steep step-like profile is characteristic of a "flipping" fiber. The tendency to flip is mollified as $\cos(L/4R)$ decreases from unity.

As a quantifier of the degree of scoop, or the tendency to migrate across streamlines during a period, it is useful to introduce the normalized total displacement D_y/L, say, across streamlines in half a period; this quantity would appear to have some significance in that it is independent of initial conditions. It is given by the explicit formula

$$\frac{D_y}{L} = \frac{1}{\sqrt{2}}\frac{R}{L}\left[\frac{\sin^2(L/4R)}{\cos(L/4R)}\right](1+\cos^2(L/4R))^{1/2}\times \\ \log\left[\frac{(1+\cos^2(L/4R))^{1/2}+2\cos(L/4R)}{(1+\cos^2(L/4R))^{1/2}-2\cos(L/4R)}\right]. \tag{87}$$

After displacing across streamlines by distance D_y in half a period a fiber then returns to its initial y-location in the second half of the period.

Figure 7 shows D_y/L as a function of $\cos(L/4R)$. As the fiber becomes straight $D_y/R \to 0$ and the "scoop" disappears. An interesting result is that a local maximum of $D_y/R \approx 0.447$ occurs for $\cos(L/4R) \approx 0.72$ which roughly corresponds to $L \approx \pi R$ so that the length of the fiber occupies approximately half its circle of curvature (see Figure 8); we deduce that such fibers have the strongest tendency to drift across streamlines. On the other hand, in the singular limit as $\cos(L/4R) \to 0$ and the two fiber end-points become very close, the scoop tends to a value close to 0.32.

Only the displacement in the streamwise direction is found to depend on initial conditions. Interestingly we have found that it is possible, by a careful choice of initial conditions, to identify *completely periodic* motions, that is, ones for which there is no net displacement of the fiber even in the streamwise direction. Figure 9 illustrates this with midpoint trajectories for three different choices of $y_c(0)$ for a given fiber with $L = 1$ and $\cos(L/4R) = 0.8$ and $\phi(0) = 0$ in each case. For $y_c(0) = 0.222$, a value found by trial and error, the trajectory of the fiber midpoint is a closed periodic orbit. Such localization phenomena are only possible for completely straight fibers if they are centred on $y = 0$ since they will otherwise translate along the streamline on which the fiber midpoint is located.

Figure 10 shows the instantaneous velocity fields, computed using (82), around a fiber with $L = 0.5$ and $R = 0.15$ at three typical points on its trajectory, including its initial configuration. Here it is easy to see the presence of a stagnation point in the flow close to the fiber; using the analytical solution (81) we determined this stagnation point to be at approximately 0.031i in the initial configuration. The presence of a recirculation zone

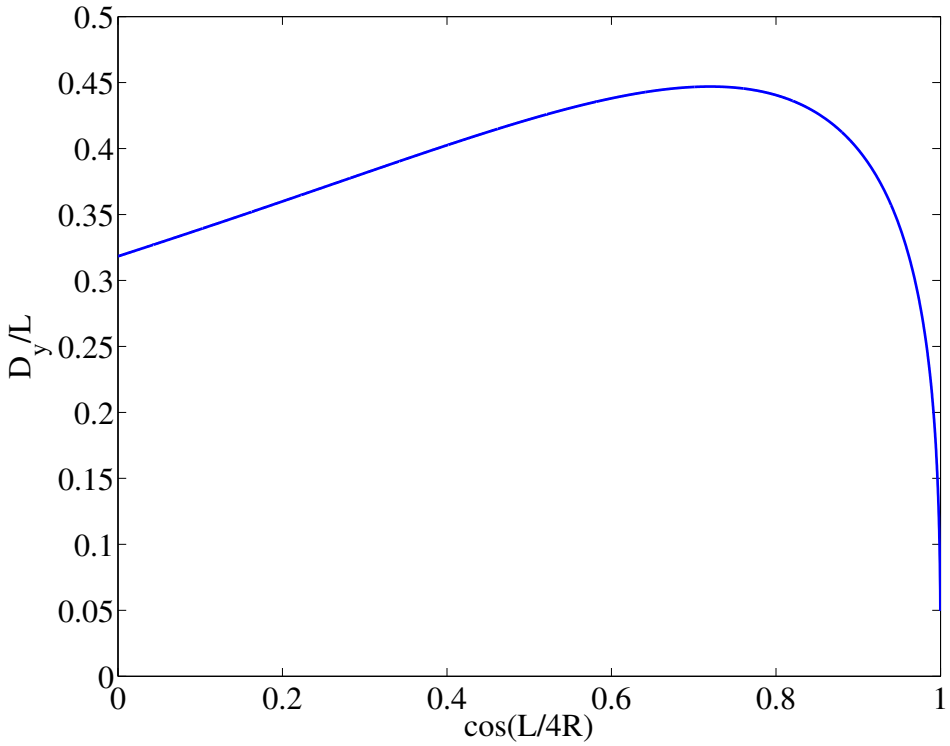


FIG. 7. The degree of "scoop": normalized displacement across streamlines D_y/L against against $\cos(L/4R)$. There is a local maximum $D_y/L \approx 0.447$ at $\cos(L/4R) \approx 0.72$.

associated with this stagnation point just north of the fiber is clear from the first quiver plot of Figure 10. As the fiber evolves so does the position of this stagnation point relative to it. Given the analytical form of the flow fields encapsulated in (82) it is easy to study such features of the velocity field in detail.

VI. CURVED FIBER IN AN EXTENSIONAL FLOW

Since it is also of interest in applications[16], we outline the analogous analysis of the curved fiber in an extensional flow (or linear straining flow) of the form

$$(u, v) \to (\dot{\delta}x, -\dot{\delta}y), \qquad \text{as } |x|, |y| \to \infty, \tag{88}$$

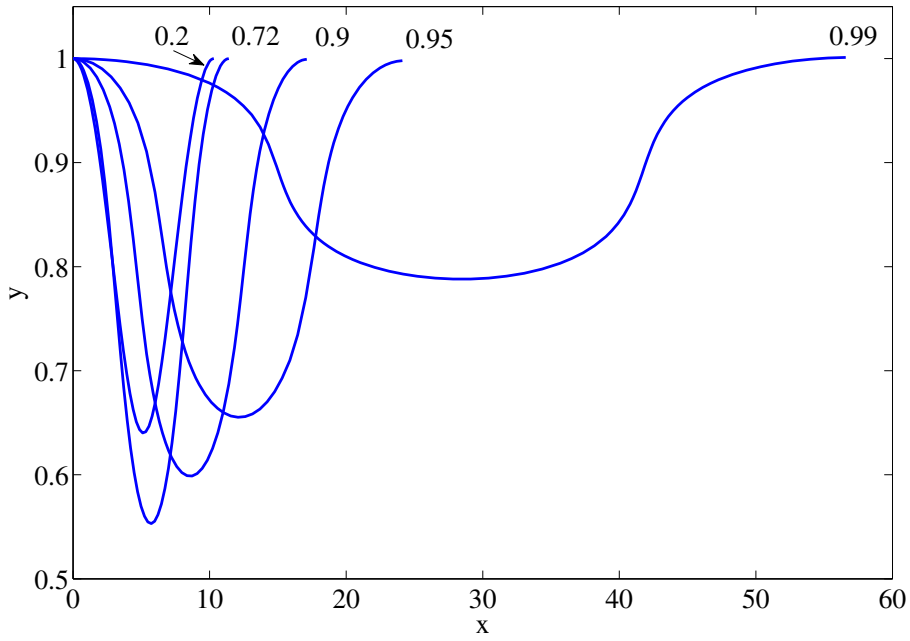


FIG. 8. Trajectories in the (x, y)-plane of the fiber midpoints placed initially at $(0, 1)$ labelled by $\cos(L/4R)$. The distance travelled in a period increases with $\cos(L/4R)$. The trajectory with $\cos(L/4R) = 0.72$ displaces most in the cross-stream direction.

where $\dot{\delta} \in \mathbb{R}$ is the far-field strain rate. Now $f(z)$ and $g'(z)$ have the modified far-field form

$$f(z) \sim f_0 + \mathcal{O}(1/z), \qquad g'(z) \sim \dot{\delta} z + g_0 + \mathcal{O}(1/z), \qquad \text{as } |z| \to \infty, \tag{89}$$

where f_0 and g_0 satisfy (12). All other aspects of the boundary value problem are the same as in the case of simple shear; in particular, the boundary condition (52) still pertains for U and Ω to be determined.

Since $f(z)$ no longer has a simple pole at infinity, $F(\zeta)$ is now analytic at $\zeta = \alpha$ and turns out, as we now show, to have the functional form

$$F(\zeta) = \frac{D}{1/\zeta - \overline{\alpha}} + \frac{E}{1/\zeta - \alpha}, \tag{90}$$

where D and E are to be determined. From (54), and substitution of (90), we find that, as

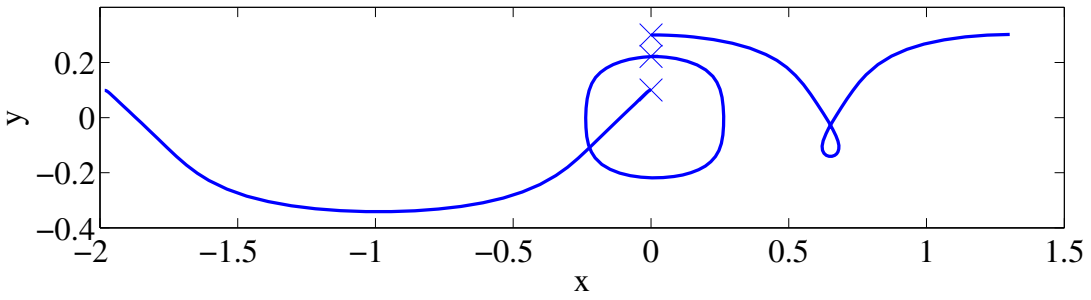


FIG. 9. Localized completely periodic motions. Orbits with $L = 1$ and $\cos(L/4R) = 0.8$ with initial conditions $\phi(0) = 0, x_c(0) = 0$ and $y_c(0) = 0.1, 0.222, 0.3$ (shown as crosses). For $y_c(0) = 0.222$ the orbit is completely periodic.

$|z| \to \infty$,

$$G(\zeta) = \overline{D}\left[\frac{z}{Q} - \frac{P}{Q} - \frac{S}{z}\right] + \overline{E}\left[\frac{1}{2\alpha} - \frac{Q}{4\alpha^2}\frac{1}{z}\right] + \overline{U} - \mathrm{i}\Omega\left[\mathrm{i}e^{-\mathrm{i}\phi}R + \frac{R^2}{z}\right] + \mathcal{O}(1/z^2). \tag{91}$$

Requiring that $g'(z)$ behaves like $\dot{\delta}z$ as $z \to \infty$ requires that

$$\frac{\overline{D}}{Q} = \dot{\delta}, \qquad \text{or} \qquad D = -2\dot{\delta}rRe^{-\mathrm{i}\phi}\left[\frac{1-r^2}{1+r^2}\right]. \tag{92}$$

The condition that the $1/z$ contribution to the far-field form (91) vanishes (the zero torque condition) implies

$$-\overline{D}S + \frac{\overline{E}Q}{4r^2} - \mathrm{i}\Omega R^2 = 0. \tag{93}$$

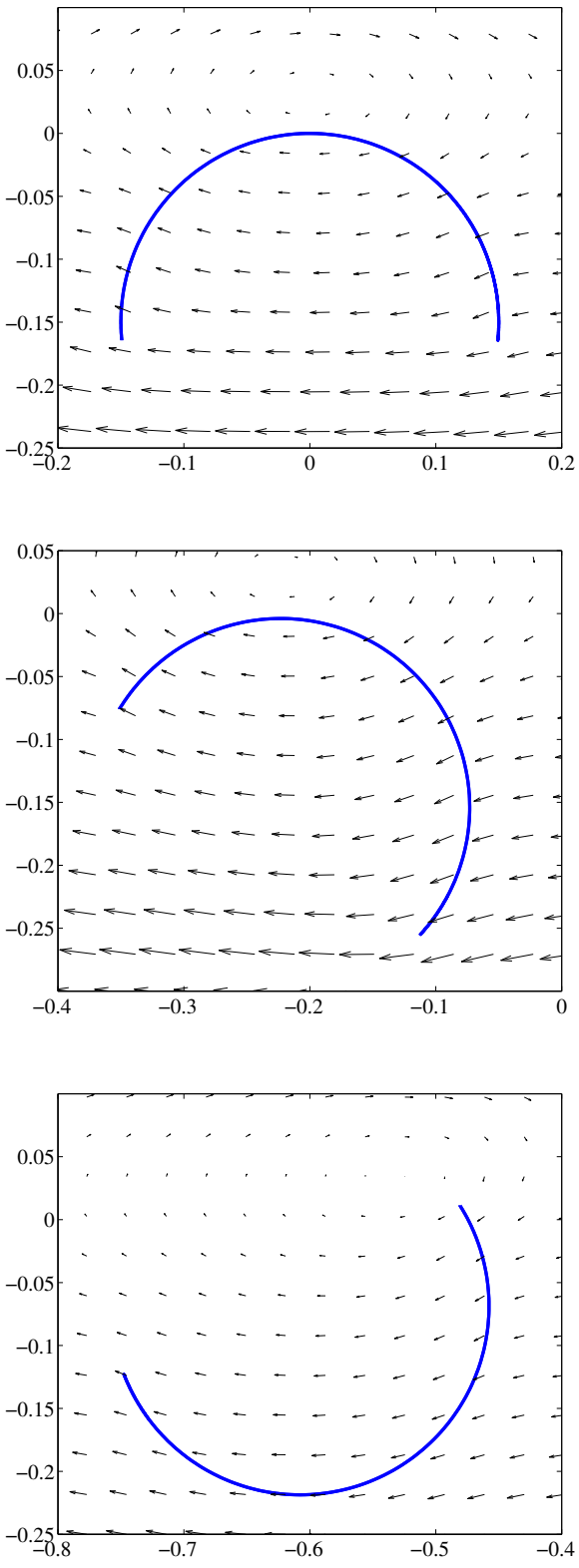


FIG. 10. Velocity fields for three configurations on the fiber trajectory in simple shear with initial conditions $z_c(0) = 0, \phi(0) = 0$ with $L = 0.5$ and $R = 0.15$. There is a stagnation point near the fiber in all three configurations. In the initial configuration (shown at top) it is at 0.031i.

The real part of this equation can be shown, after some algebra, to yield

$$\mathrm{Re}[\overline{E}e^{\mathrm{i}\phi}] = -\frac{4\dot{\delta}r^3R(1-r^2)}{(1+r^2)^3}\left[e^{2\mathrm{i}\phi}+e^{-2\mathrm{i}\phi}\right]. \tag{94}$$

As for simple shear we find an equation for the imaginary part of $\overline{E}e^{\mathrm{i}\phi}$ by examining the condition that the pole of $G(\zeta)$ at $\overline{\alpha}$ is removable. Algebraic manipulations result in

$$\mathrm{Im}[\overline{E}e^{\mathrm{i}\phi}] = -\mathrm{i}\dot{\delta}rR\left[\frac{1-r^2}{1+r^2}\right]^3\left[e^{2\mathrm{i}\phi}-e^{-2\mathrm{i}\phi}\right]. \tag{95}$$

Together (94) and (95) imply

$$\overline{E}e^{\mathrm{i}\phi} = -\frac{4\dot{\delta}r^3R(1-r^2)}{(1+r^2)^3}\left[e^{2\mathrm{i}\phi}+e^{-2\mathrm{i}\phi}\right] + \dot{\delta}rR\left[\frac{1-r^2}{1+r^2}\right]^3\left[e^{2\mathrm{i}\phi}-e^{-2\mathrm{i}\phi}\right]. \tag{96}$$

Use of this in (93) implies that

$$\Omega = -\dot{\delta}\left[\frac{1-r^2}{1+r^2}\right]^2\sin 2\phi = -\dot{\delta}\cos^2\left(\frac{L}{4R}\right)\sin 2\phi. \tag{97}$$

From (91) we identify

$$g_0 = -\frac{\overline{D}}{Q}P - \frac{\mathrm{i}\overline{E}}{2r} + \overline{U} + \Omega Re^{-\mathrm{i}\phi} \tag{98}$$

while evaluation of (90) at $\zeta = \alpha = \mathrm{i}r$ yields

$$f_0 = \frac{\mathrm{i}Dr}{1-r^2} + \frac{\mathrm{i}Er}{1+r^2}. \tag{99}$$

Condition (12) then implies that

$$U = \dot{\delta}\overline{z_c} + \mathrm{i}\dot{\delta}Re^{-\mathrm{i}\phi}\left[1-\cos^4\left(\frac{L}{4R}\right)\right]. \tag{100}$$

Finally, (97) and (100) lead to the system (2) reported earlier.

In the limit $L/(4R) \to 0$, corresponding to a straight fiber, we find the system

$$\frac{dz_c}{dt} = \dot{\delta}\overline{z_c}, \qquad \frac{d\phi}{dt} = \Omega = -\dot{\delta}\sin 2\phi. \tag{101}$$

This same result can be obtained by modifying (to an extensional flow) the analysis based

on use of the standard Joukowski map presented in §III for the case of simple shear. In the limit $L/(4R) \to 2\pi$, corresponding to a circular disc, we find the system

$$\frac{d\phi}{dt} = \Omega = 0, \qquad \frac{dz_c}{dt} = \dot{\delta}\overline{z_c} + \mathrm{i}\dot{\delta}Re^{-\mathrm{i}\phi}. \tag{102}$$

But

$$c = z_c - \mathrm{i}Re^{\mathrm{i}\phi}, \qquad \text{hence} \qquad \frac{dc}{dt} = \frac{dz_c}{dt} = \dot{\delta}\overline{c} \tag{103}$$

so the system for c and ϕ is

$$\frac{dc}{dt} = \dot{\delta}\overline{c}, \qquad \frac{d\phi}{dt} = 0 \tag{104}$$

which is easily verified to be the system governing the center and orientation of a circular disc with in an extensional flow.

VII. DISCUSSION

The Jeffery-type dynamical system for the evolution of curved 2D rigid fibers in simple shear, and in an extensional flow, at low Reynolds numbers has been derived. The equations are given in closed form, and include a full resolution of the end-point singularities. Beyond the well-known results for ellipsoids[1,5], we are not aware of any other analytical characterizations of such Jeffery-type systems so we believe our results are a valuable addition to the literature. Unlike a straight fiber, which can be derived as a limiting case of an ellipsoid, a curved fiber can not be derived in any such limit. Our analysis therefore offers genuinely new results. We have also solved for the full flow-field, as given for example in (82), associated with the evolving fibers and this should be valuable in its own right (for example, as a check on boundary integral or other numerical formulations).

A detailed study of the ordinary differential equations lends insights into the dynamical phenomena recently dubbed "flipping" and "scooping" by other authors[15] who carried out a computational study of curved rigid fibers (in the fully three dimensional case) using approximating computational models. The "drift" phenomenon also observed by those authors is not captured within our two-dimensional model since it is an essentially out-of-shear-plane effect. Our analytical results should provide valuable benchmark tests for computational studies in the rigid fiber limit.

The results here concern curved 2D fibers but, on the basis of the fact that it is true for *straight* 2D fibers, we expect that equations (1) will also govern the motion of curved 3D fibers evolving purely in the plane of shear; similarly, (2) should govern the motion of 3D fibers evolving purely in the extensional flow plane. It should be possible to confirm all this using slender body theory.

Acknowledgments: The author acknowledges support from an Established Career Fellowship from EPSRC (EP/K019430/1) and a Research Grant from The Leverhulme Trust in the UK.

REFERENCES

[1]G. B. Jeffery, The motion of ellipsoidal particles immersed in a viscous fluid, *Proc. Roy. Soc. A*, **102**, 161, (1922).

[2]F. P. Bretherton, The motion of rigid particles in a shear flow at low Reynolds number, *J. Fluid Mech.*, **14**, 284, (1962).

[3]D. G. Crowdy & O. Samson, Stokes flow past gaps in a wall, *Proc. Roy. Soc. A*, **466**, 2727-2746, (2010).

[4]C. Duprat & H. Stone (Eds), Fluid-structure interactions in low-Reynolds-number flows, Royal Society Soft Matter Series, The Royal Society (London), (2015).

[5]E. J. Hinch & L. G. Leal, Rotation of small non-axisymmetric particles in a simple shear flow, *J. Fluid Mech.*, **92**, 591, (1979).

[6]P. Skjetne, R. F Ross & D. J. Klingenberg, Simulation of single fiber dynamics. *J. Chem. Phys.*, **107**, 2108–2121, (1997).

[7]A. L. Yarin, O. Gottlieb & I. V. Roisman, Chaotic rotation of triaxial ellipsoids in simple shear flow, *J. Fluid Mech.*, **340**, 83, (1997).

[8]M. Makino & M. Doi, Migration of twisted ribbon-like particles in simple shear flow, *Phys. Fluids*, **17**, 103605, (2005).

[9]B. J. Treyelyan & S. G. Mason, Particle motions in sheared suspensions. I. Rotations, *J. Colloid Sci.*, **6**, 354, (1951).

[10]J. Happel & H. Brenner, Low Reynolds number hydrodynamics, Martinus Nijhoff, The Hague, (1983).

[11]S. Kim & S. J. Karrila, Microhydrodynamics, Butterworth-Heinemann, Stoneham, (1991).

[12]S. Yamamoto & T. Matsuoka, A method for dynamic simulation of rigid and flexible fibers in a flow field, *J. Chem. Phys.*, **98**, 644–650, (1993).

[13]A. K. Tornberg & M. J. Shelley, Simulating the dynamics and interactions of flexible fibers in Stokes flows, *J. Comput. Phys.* **196**, 8–40, (2004).

[14]J. K. Wiens & J. M. Stockie, Simulating flexible fiber suspensions using a scalable immersed boundary algorithm, *Comput. Methods Appl. Mech. Engrg.*, **290**, 1-18, (2015).

[15]J. Wang, E. J. Tozzi, M. D. Graham & D. J. Klingenberg, Flipping, scooping, and spinning: Drift of rigid curved nonchiral fibers in simple shear flows, *Phys. Fluids*, **24**, 123304, (2012).

[16]H. Manikantan & D. Saintillan, Buckling transition of a semiflexible filament in extensional flow *Phys. Rev. E*, **92**, 041002(R), (2015).

[17]N. Quennouz. M. Shelley, O. du Roure and A. Lindner, Transport and buckling dynamics of an elastic fibre in a viscous cellular flow, *J. Fluid Mech.*, **769**, 387–402, (2015).

[18]W.E. Langlois, Slow viscous flows, Macmillan, New York, (1964).

[19]D.G. Crowdy & S. Tanveer, A theory of exact solutions for plane viscous blobs, *J. Nonlinear Sci.*, **8**(3), 261-279, (1998).

[20]W. R. Dean and P. E. Montagnon, On the steady motion of viscous liquid in a corner, *Proc. Camb. Phil. Soc*, **45**, 389, (1949).

[21]H. K. Moffatt, Viscous and resistive eddies near a sharp corner, *J. Fluid Mech.*, **18**, 1–18, (1964).

[22]A. H. England, Complex variable methods in elasticity, Dover, New York, (2003).

[23]H. Hasimoto, On the flow of a viscous fluid past a thin screen at small Reynolds numbers, *J. Phys. Soc. Japan*, **13**(6), 633–639, (1958).

[24]S. H. Smith, Stokes flow past slits and holes, *Int. J. Multiphase Flow*, **13**(2), 219–231, (1987).

[25]H-J. Ko & J-T Jeong, Two-dimensional slow stagnation flow near a slit, *J. Phys. Soc. Jap.*, **63**(9), 3288–3294, (1994).

[26]H. Hasimoto, Creeping viscous ow past a circular arc with special reference to separation, *J. Phys. Soc. Japan*, **47**, 347–348, (1979).

[27]D. G. Crowdy, Conformal slit maps in applied mathematics, *ANZIAM Journal*, **53**(3), 171-189, (2012).

[28]P. J. Davis, The Schwarz function and its applications, Carus Mathematical Monographs,

Wiley and Sons, (1978).

[29]D. G. Crowdy, Exact solutions for cylindrical "slip-stick" Janus swimmers in Stokes flow, *J. Fluid Mech.*, **719**, R2, (2013).